INFRASONIC OBSERVATIONS OF LARGE-SCALE HE EVENTS

Rodney W. Whitaker, J. Paul Mutschlecner,
Masha B. Davidson, and Susan D. Noel

Los Alamos National Laboratory

INTRODUCTION

The Los Alamos Infrasound Program has been operating since about mid-1982, making routine measurements of low frequency atmospheric acoustic propagation. Generally, we work between 0.1 Hz to 10 Hz; however, much of our work is concerned with the narrower range of 0.5 to 5.0 Hz. Two permanent stations, St. George, UT, and Los Alamos, NM, have been operational since 1983, collecting data 24 hours a day. For the purposes of this discussion, we will concentrate on our measurements of large, high explosive (HE) events at ranges of 250 km to 5330 km. Because our equipment is well suited for mobile deployments, we can easily establish temporary observing sites for special events. The measurements in this report are from our permanent sites, as well as from various temporary sites. In this short report we will not give detailed data from all sites for all events; rather, we will present a few observations that are typical of the full data set.

The Defense Nuclear Agency sponsors these large explosive tests as part of their program to study airblast effects. A wide variety of experiments are fielded near the explosive by numerous Department of Defense (DOD) services and agencies. Our measurement program is independent of this work; we use these tests as energetic known sources, which can be measured at large distances. Ammonium nitrate and fuel oil (ANFO) is the specific explosive used by DNA in these tests. Table I gives the test names, dates, charge weights, and number of our infrasonic stations operated for each test. All tests were fired at White Sands Missile Range, NM.

BACKGROUND

The basic sensor for our work is the Globe 100 microphone. A series of porous hoses is used to reduce the noise from the low-level local wind. Figure 1 shows a microphone and associated noise-reducing hoses, which can be thought of as a modification of the Daniel's tube used for lower frequency work (reference 1). During periods of quiet background, this sensor can easily detect signals down to a few tenths of a microbar. In our frequency

domain, there are natural as well as man-made sources of infrasound, some of which are described in Chapter 9 of reference 2. However, this background is not saturated with confusing signals, which simplifies the detection problem considerably.

An infrasound array consists of 3 to 6 sensors placed in a regular pattern. We employ standard, time-delay, and sum beamforming techniques to process the recorded data. The present algorithm is a modified version of one due to Young and Hoyle (reference 3). Generally, 20-seconds of data are processed at a time, followed by a 50% shift and continued processing. For each 20-second window, the beamformer provides the correlation coefficient, trace velocity, and azimuth of the highest correlation signal, as well as the power spectrum for that interval. Longer intervals of data can be summarized in the manner illustrated in figure 2, where 60 minutes of data are shown. The presence of a signal is easily seen as the fixed azimuth line from 16:36 UT to 16:43 UT.

Signal energy propagates in the atmospheric sound ducts created by the ambient temperature structure, or by a combination of temperature and wind. When propagation is in the same direction as the upper atmospheric winds, total refractions occur between 40 km and 60 km altitudes. The upper atmospheric winds are seasonal in nature, blowing to the east in winter and to the west in the summer (reference 4). It is important to note that at these altitudes the wind speed can be a significant fraction of the sound speed; therefore, the wind profile must be included correctly in any calculational work. The simplification of an effective sound speed profile is not appropriate for these propagation paths.

OBSERVATIONS

Before discussing specific time series for two events, a few general comments will be useful. We use the concept of an average velocity to broadly classify the observed propagation paths. Here, average velocity is just the great circle source to receiver distance divided by travel time. With wind propagation, the strongest signals arrive with an average velocity of 0.29 km/s. Ray tracing results confirm that this corresponds to total refractions at 40 km to 60 km altitudes. Higher average velocities indicate lower paths, and conversely. The stations north and northwest of White Sands, Los Alamos and St. George, often observe a first arrival with an average velocity of 0.34 km/s. This must be energy that travels at or very near the surface; we will for the moment refer to this as the surface wave.

The seasonal winds have a significant effect on observed pressures. A propagation path in the direction of the wind will result in a larger pressure than along a path directed against the wind. We apply a correction for this effect, which normalizes amplitudes to a zero wind condition. This procedure is described in reference 5.

For the Minor Scale test we had two arrays at Barking Sands, Kauai, HI, at a distance of 5330 km, our most distant detection. One array operated at our standard frequency range, while the other operated at lower frequency, about 0.01 Hz to 0.1 Hz. Both arrays detected the event, but the detection at the lower frequency was much better, as expected for such large distances.

Figure 3 presents single channel time series from four sites for the Misty Picture event. Each panel is composed of 12 minutes of data in three, four minute windows. The time above each window is the time at the start of the window. Average velocities, m/s, are written below specific features for easy reference. For Los Alamos, note the surface wave at 342.5 m/s. For these time series, the data are well correlated with the source azimuth from first arrival to the end of the record shown.

Figure 4 is the same as figure 2 but is for the Misers Gold event. The surface wave at Los Alamos is evident with a 339.2 m/s average velocity. Again signal energy is well-correlated with source azimuth from first arrival until the end of the displayed record. These two figures illustrate the character of the observations for these energetic events. Strong multiple arrivals are common, with total durations on the order of 10 minutes. The surface wave is common at 250 km north, and has been observed at 750 km to the northwest.

In figure 5, power spectra contours are shown for the Misty Picture event as observed at St. George, UT. Contours of power are given as functions of time and frequency. Four major arrivals are seen from 18:56:30 to 19:03:00, with the largest powers concentrated below 1.2 Hz. Note that the major arrivals have frequency contributions across the whole band, from 0.2 Hz to 3.0 Hz.

For the purpose of examining pressure as a function of range, we have found it useful to place all the data on a common scale by the use of scaled range. In figure 6, we give the peak-to-peak amplitude of the largest signal (wind corrected) as a function of scaled range. The scaled range is the actual range divided by $(2W)^{1/2}$, where W is the charge weight in tons, the factor of

2 is the standard factor for surface explosions, and the exponent is that appropriate for the cylindrical geometry of the ducted paths. The least squares slope is -1.4, showing only a modest increase in loss over the cylindrical value of -1.0.

During the conference, a few of the participants (Drs. Raspet, Attenborough, and West) suggested that the surface wave was likely a creeping wave, as described by Pierce (reference 6). Following the discussion in reference 6, we have estimated the attenuation for such waves and find an attenuation coefficient of 0.1 km^{-1}. Over the shorter path of 250 km, this gives a huge loss, sufficiently large, we believe, to rule out this explanation.

We wish to acknowledge the support of the Department of Energy Office of Arms Control for the work supported here.

TABLE I - EXPERIMENTS

Event	Date	Weight Tons	Sites
Millrace	9/16/81	600	1
Pre Direct Course	10/7/82	24	2
Direct Course	10/26/83	600	4
Minor Scale	6/27/85	4800	4
Misty Picture	5/14/87	4800	5
Misers Gold	6/01/89	2400	8

REFERENCES

1. Daniels, F. B.: Noise Reducing Line Microphone for Frequencies Below 1 cps. JASA 31, 529-531, 1959.

2. Gossard, Earl E.; Hooke, William H.: Waves in the Atmosphere. Elseview Sci. Pub. Co., 1975, Ch. 9.

3. Young, Jessie M.; Hoyle, Wayne A.: Computer Programs for Multidimensional Spectra Array Processing. NOAA Technical Report ERL 345-WPL43, 1975.

4. Webb, Willis L: Structure of the Stratosphere and Mesosphere. Academic Press, 1966.

5. Mutschlecner, J Paul; Whitaker, Rodney W.: The Correction of Infrasound Signals for Upper Atmospheric Winds. Fourth International Symposium on Long Range Sound Propagation, NASA CP-3101, 1990.

6. Pierce, Allan D.: Acoustics: An Introduction to Its Physical Principles and Applications. McGraw-Hill, Inc. 1981.

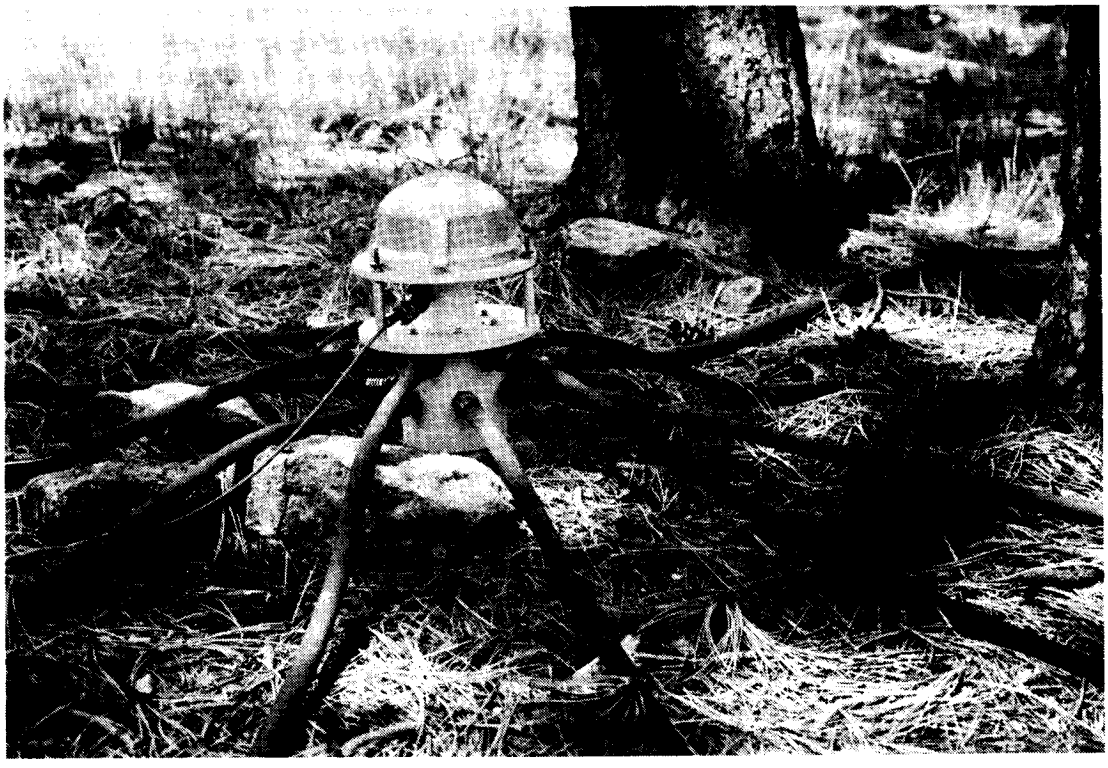

Figure 1. Infrasound microphone and noise reducing porous hoses.

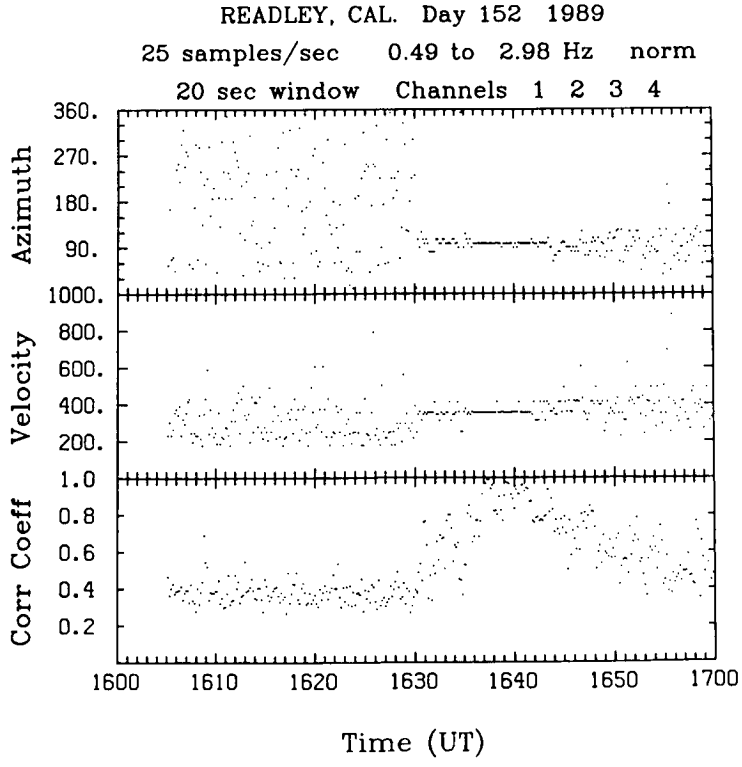

Figure 2. Summary of beamformer array processing program showing correlation coefficient, trace velocity, and azimuth as functions of time. Data are for Miser's Gold event observed at Readley, Ca.

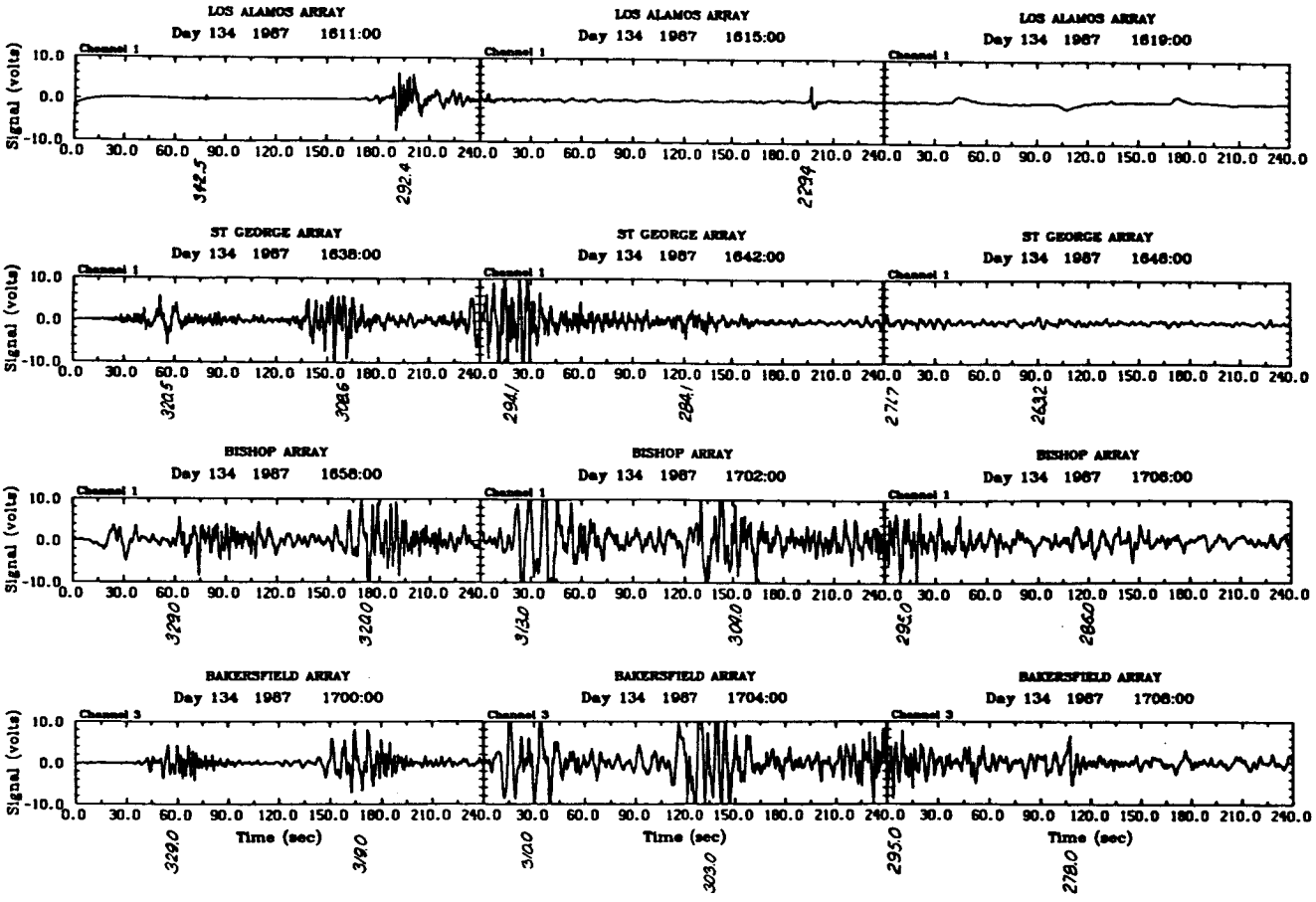

Figure 3. Samples of observed Misty Picture time series from four stations. The Bishop and Bakersfield stations were in California.

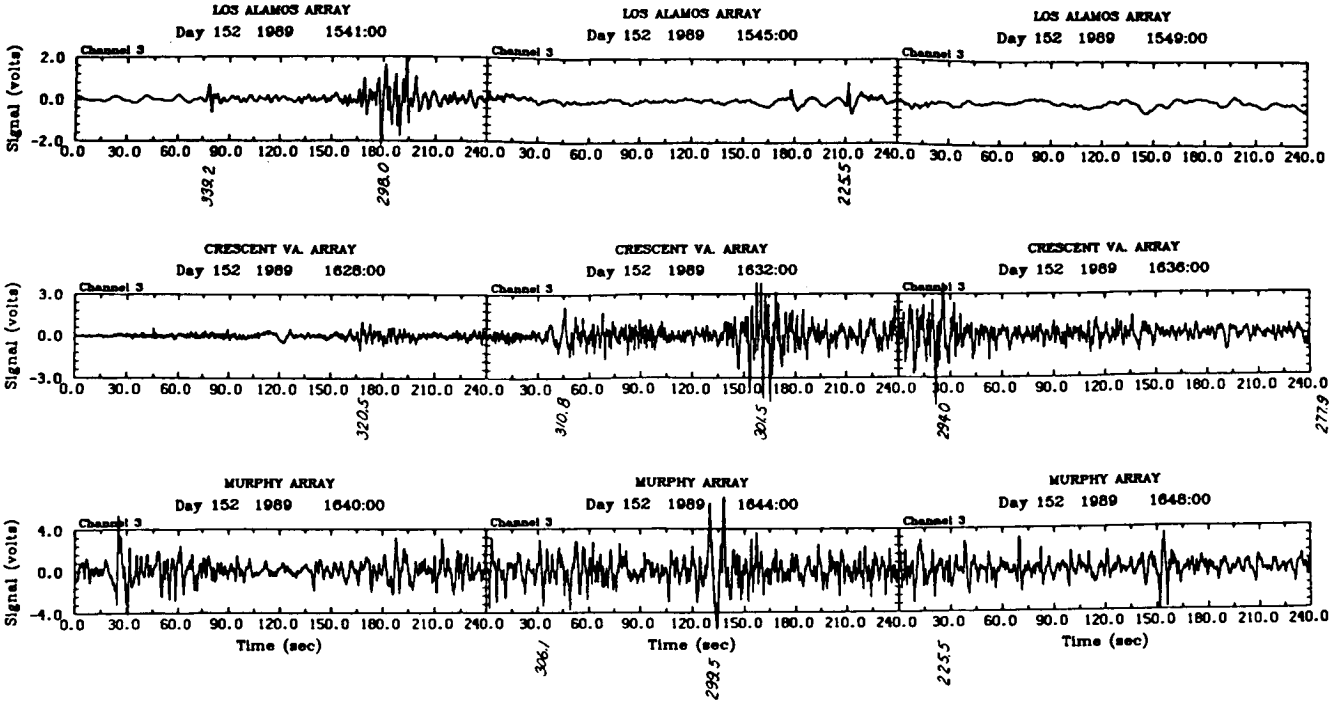

Figure 4. Samples of observed Miser's Gold time series from three stations. Crescent Valley is in Nevada, and Murphy is in Idaho.

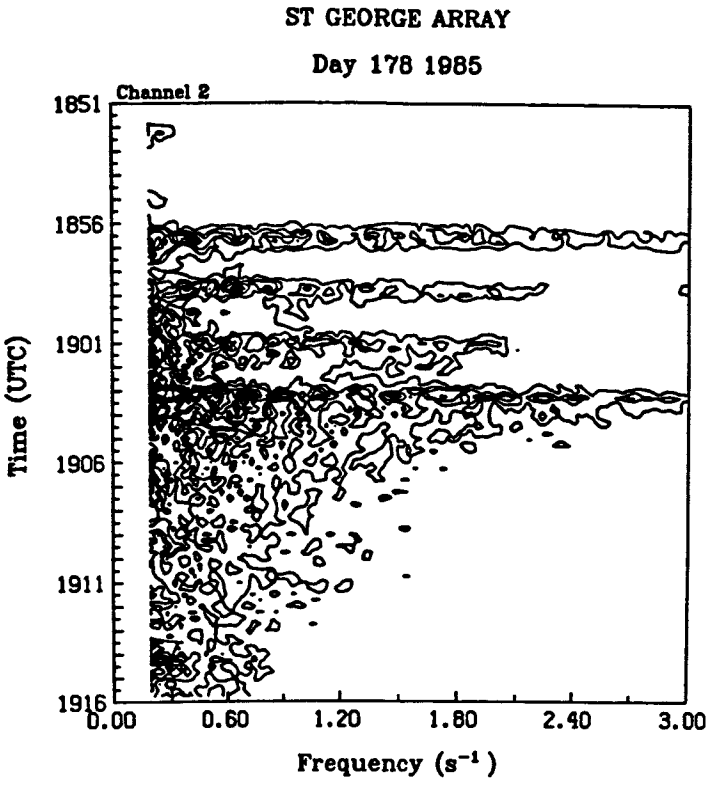

Figure 5. Power spectra contours for Misty Picture from the St. George, UT array.

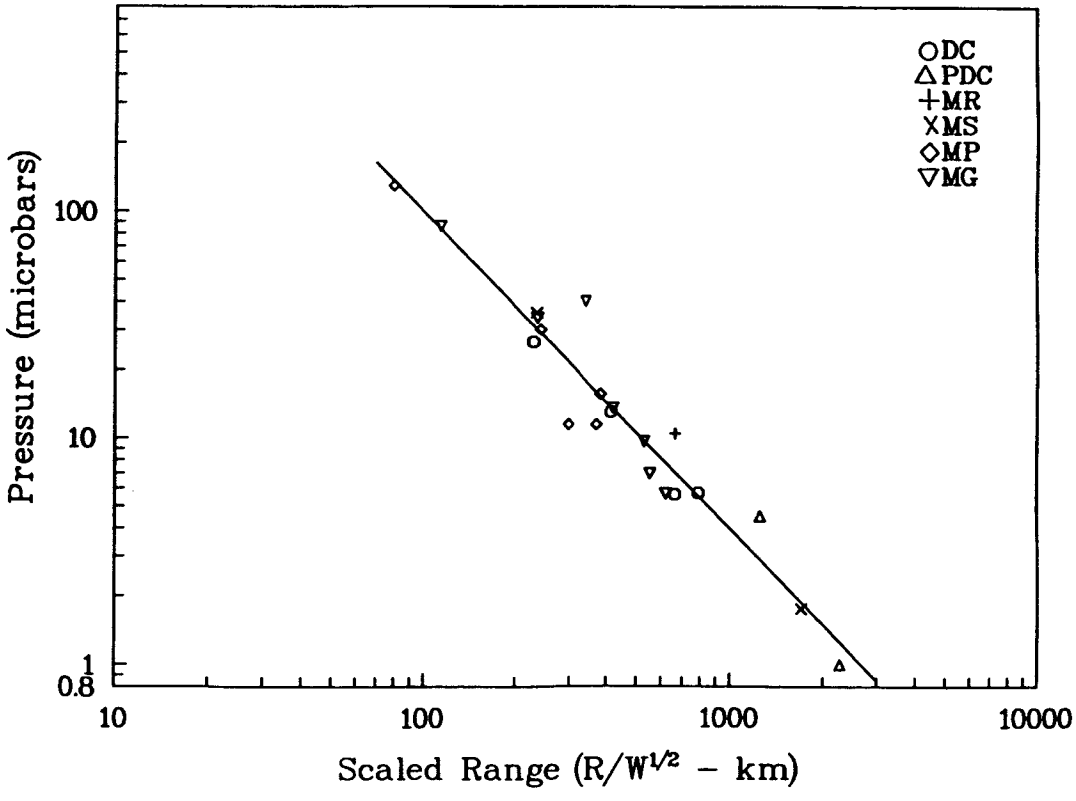

Figure 6. Peak to peak amplitude vs scaled range for the six HE events.